

**Nanosecond-scale hot-carrier cooling dynamics in one-dimensional quantum dot superlattices**Yukihiro Harada,<sup>\*</sup> Naofumi Kasamatsu, Daiki Watanabe, and Takashi Kita*Department of Electrical and Electronic Engineering, Graduate School of Engineering, Kobe University, 1-1 Rokkodai, Nada, Kobe 657-8501, Japan*

(Received 2 November 2015; revised manuscript received 12 February 2016; published 8 March 2016)

We report the time-resolved photoluminescence spectroscopy of nanoseconds-scale hot-carrier (HC) cooling dynamics in InAs/GaAs quantum dot superlattices (QDSLs). We demonstrate supra 1000-K time-averaged carrier temperature in the InAs/GaAs QDSLs from one-dimensional density of states restricting the phase space and energy-momentum conservation in the carrier scattering processes. The InAs/GaAs QDSLs HC energy dissipation rate was much smaller than that for InAs/GaAs multiple quantum wells and nearly excitation-photon-density independent, implying reduced efficiency of carrier-carrier scattering.

DOI: [10.1103/PhysRevB.93.115303](https://doi.org/10.1103/PhysRevB.93.115303)**I. INTRODUCTION**

Optically excited hot carriers (HCs) in semiconductors provide electrical and optical extraction routes for improving the energy efficiency of solar cells (SCs) [1–5] and photodetectors [6] beyond the band-gap spectral limit. Carrier thermalization typically occurs in a few picoseconds [7,8]; therefore, an HC absorber material should reduce the carrier cooling rate towards the radiative recombination time scale of nanoseconds, especially for HCSCs [2,9]. Quantum structures, such as quantum wells (QWs), quantum wires (QWRs), and quantum dots (QDs), are promising for reducing the carrier cooling rate [9–13]. In particular, the phonon bottleneck effect in QDs, observed only in a narrow window of diameters [14], induces slow electron cooling on the nanoseconds time scale [11].

On the other hand, heat leakage to the contacts occurs when HCs are extracted from the absorber in HCSCs. This energy loss mechanism can be minimized by using an energy selective contact with a narrow range of transmitted energies [2]. Conversely, spectrally broad semiselective contacts are compatible with an efficiency exceeding the single-junction conversion limit (the so-called Shockley-Queisser limit) [15]. Recently, HC photocurrent extraction in InGaAs/GaAs QWSCs has been demonstrated at 10 K and forward bias of 1.2 V [16]. Furthermore, the quasi-Fermi level splitting at the barrier energy has been demonstrated to exceed the absorption threshold of the InGaAsP QWs at 300 K, indicating a working condition of the HCSCs [17]. These results suggest that semiconductor heterostructures act as both HC absorbers and energy selective contacts.

The HC cooling rate in QWRs is slower than that in QWs [18,19], as a consequence of the restrictions of phase space and energy-momentum conservation in the scattering processes [20,21]. Besides, a one-dimensional QD superlattice (QDSL) is expected to reduce the optical phonon scattering when the miniband is narrower than the optical phonon energy [22]. The miniband width in QDSLs can be controlled by the spacer layer thickness in between stacked QDs and by the number of stacking layers. Recently, we have proposed an HCSC utilizing InAs/GaAs QDSLs, and demonstrated that

the carrier temperature in the InAs/GaAs QDSLs increases more significantly than in QWs and bulk crystals, owing to the one-dimensional density of states [23]. In the present paper, we report a remarkably reduced HC energy dissipation rate in one-dimensional InAs/GaAs QDSLs, estimated by using time-resolved photoluminescence (PL) spectroscopy. Nanoseconds-scale HC cooling dynamics were clearly observed in epitaxial quantum structures. Here, it is noted that the *continuum* density of states in the QDSLs are essential for discussing the hot-carrier cooling dynamics, because the discrete density of states in the decoupled QDs determine the carrier dynamics only by the state filling.

**II. EXPERIMENTAL**

InAs/GaAs QDSLs were grown on a semi-insulating GaAs(001) substrate by using solid-source molecular-beam epitaxy [23–25]. After thermally cleaning the substrate, a 400-nm-thick GaAs buffer layer was grown at 550 °C. Nine replicas of the InAs QD layer and the GaAs spacer layer were alternately grown at 480 °C. The nominal thicknesses of InAs and GaAs were 2.0 monolayers (MLs) and 5.2 nm, respectively. The process was interrupted for 10 s after growing each GaAs spacer layer. Finally, a 100-nm-thick GaAs capping layer was deposited. The beam-equivalent pressure of the As<sub>2</sub> flux was  $1.3 \times 10^{-3}$  Pa. The GaAs spacer layer thickness of 5 nm is sufficiently thin to couple the electronic states along the stacking direction and to form a miniband [24]. The QDSL density was approximately  $2 \times 10^{10}$  cm<sup>-2</sup>. Conversely, at low temperatures (<~20 K), the miniband is not formed in the fundamental state because the energy states within the homogeneous energy width can couple one with another [24]. The homogeneous linewidth of the excited state is more than one order of magnitude larger than that of the fundamental state [26]. Therefore, the excited state easily causes miniband formation even at low temperatures [27]. These results suggest that the fundamental states of the QDs are not *completely* coupled with each other below ~20 K. However, it is obvious that the PL decay lifetime in the low-temperature region below ~20 K increases with increasing the superlattice period [24], suggesting the exciton wave function of the fundamental state delocalizes in the QDSLs. Besides, the linearly polarized PL spectra of the InAs/GaAs QDSLs used in this study show an anisotropy of

<sup>\*</sup>y.harada@eedept.kobe-u.ac.jp

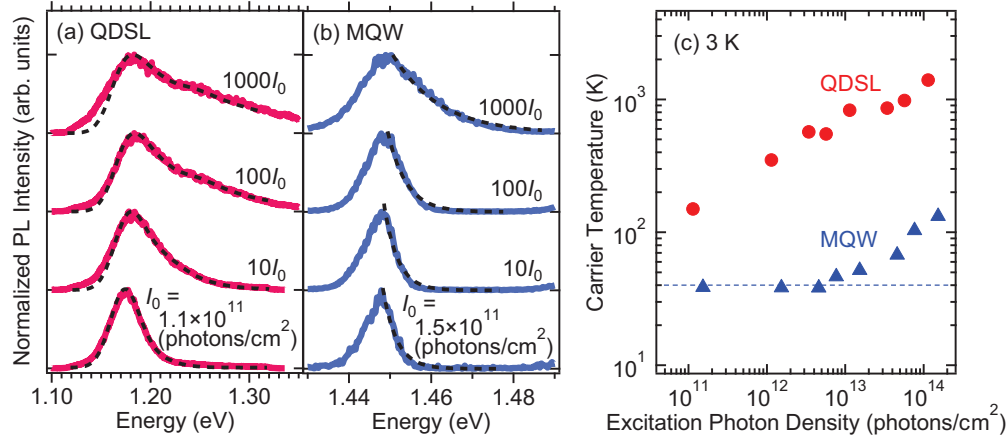


FIG. 1. Excitation-photon-density dependence of the time-integrated PL spectra of the (a) InAs/GaAs QDSLs and (b) MQWs at 3 K. The dashed black lines indicate calculated spectral line shapes for the PL spectra. (c) Time-averaged carrier temperature as a function of the excitation photon density. The dashed line is the lower limit on the estimated carrier temperature owing to the inhomogeneous broadening in the InAs/GaAs MQWs.

$(I_{E//[-110]} - I_{E//[110]}) / (I_{E//[-110]} + I_{E//[110]}) = 47\%$  at 16 K. This strong polarization anisotropy indicates that the electronic states of the InAs/GaAs QDSLs are no longer those of the decoupled QDs [25]. For these reasons, we assumed that the fundamental state of the QDSLs has the one-dimensional density of states even at low temperature. As a reference sample, we grew InAs/GaAs multiple QWs (MQWs). Ten replicas of the InAs QW layer and the GaAs spacer layer were alternately grown. Nominal InAs and GaAs depositions were 1.4 MLs and 10 nm, respectively. The InAs deposition of 1.4 MLs is thinner than the critical thickness for forming the QDs [28], and the GaAs spacer layer thickness of 10 nm is sufficiently thick to prevent the electronic coupling between the QWs. The process was interrupted for 10 s after growing each QW layer, for improving the flatness of QWs.

Time-resolved PL measurements were performed at 3 and 300 K by using a mode-locked Ti:sapphire pulse laser. The pulse duration and repetition rate were 140 fs and 80 MHz, respectively. The excitation energies were set to 1.55 and 1.65 eV for the InAs/GaAs QDSLs and MQWs, respectively. These excitation energies exceed the band-gap energy of 1.519 eV at 0 K in GaAs. The PL signal was detected by using a near-infrared streak camera system (Hamamatsu, C11293-01) for the InAs/GaAs QDSLs and by using a visible streak camera system (Hamamatsu, C5680-14) for the InAs/GaAs MQWs.

### III. RESULTS AND DISCUSSIONS

Figures 1(a) and 1(b) show the dependence of the time-integrated PL spectra of the InAs/GaAs QDSLs and MQWs, respectively, on the excitation-photon density, for the lattice temperature  $T_l$  of 3 K. At high energies, the spectral slope becomes more gradual and exhibits an obvious tail structure towards higher energies, for both samples. This is attributed to the HC distribution [17,23,29]. The carrier temperature  $T_c$  in the InAs/GaAs QDSLs was estimated by fitting to the spectral line shape, taking into account the Boltzmann factor, the one-dimensional density of states, and inhomogeneous broadening in the InAs/GaAs QDSLs [23]. We estimated the inhomogeneous Gaussian linewidth to be 33 meV according

to the full width at half maximum of the PL spectrum at 4 K under the low excitation photon density of  $1.1 \times 10^{10}$  photons/cm<sup>2</sup>. A product of the one-dimensional density of states and Boltzmann factor,  $E^{-1/2} \times \exp(-E/k_B T_c)$ , was convoluted with the Gaussian profile for the fundamental, first-excited, and second-excited sub-band transitions. Here,  $k_B$  is the Boltzmann constant. The dashed black lines represent the fitting results. The time-integrated PL spectrum was satisfactorily reproduced by varying the carrier temperature for all of the excitation photon densities. For the InAs/GaAs MQWs, the carrier temperature was simply estimated from the spectral slope in the high-energy region by using the Boltzmann factor, as shown by the dashed black lines in Fig. 1(b).

Figure 1(c) shows the time-averaged carrier temperature as a function of the excitation photon density. The dashed line is the lower limit on the estimated carrier temperature owing to the inhomogeneous broadening in the InAs/GaAs MQWs. The carrier temperature in the InAs/GaAs QDSLs was higher than that in the InAs/GaAs MQWs, for all of the excitation photon densities. The carrier temperature monotonically increased with increasing the excitation photon density, and exceeded 1000 K in the InAs/GaAs QDSLs for the excitation photon density of  $\sim 10^{14}$  photons/cm<sup>2</sup>. On the other hand, the carrier temperature of  $\sim 100$  K in the InAs/GaAs MQWs for the excitation photon density of  $\sim 10^{14}$  photons/cm<sup>2</sup> is comparable to the reported value for InGaAs/GaAsP MQWs for the excitation power density on the order of kW/cm<sup>2</sup> and sub-barrier excitation. The high carrier temperature in the QDSLs suggests the effects of the one-dimensional density of states that impose the restrictions of phase space and energy-momentum conservation in the carrier scattering processes [18–21].

A similar fitting procedure was performed for the time-resolved PL spectrum. Figures 2(a) and 2(b) show the HC cooling dynamics of the InAs/GaAs QDSLs and MQWs, respectively, for various excitation photon densities. In the InAs/GaAs QDSLs, high carrier temperature ( $>1000$  K) was maintained over 1 ns following the excitation for the

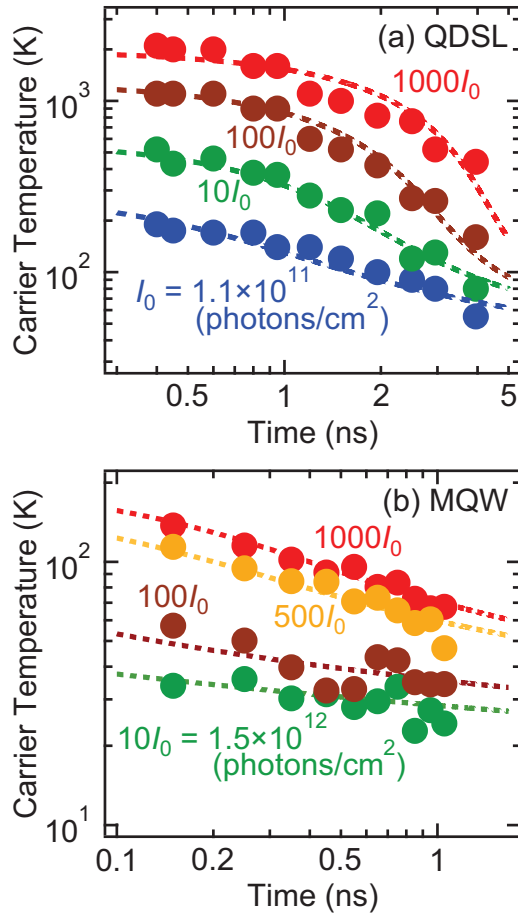


FIG. 2. HC cooling dynamics of the (a) InAs/GaAs QDSL and (b) MQWs for various excitation photon densities at 3 K. The dashed lines represent the calculated curves.

excitation photon density of  $\sim 10^{14}$  photons/cm<sup>2</sup>. On the other hand, for both the samples, the HC cooling dynamics depended on the excitation photon density. To analyze the HC cooling dynamics, we theoretically calculated the HC energy dissipation rate  $\langle dE/dt \rangle$  in carrier-phonon scattering processes, by taking into account the deformation potential scattering, piezoelectric scattering, and polar optical phonon scattering [30]. The energy dissipation rate by polar optical phonon scattering is predominant when  $T_c - T_l > \sim 30$  K, and is given as [30]

$$\left\langle \frac{dE}{dt} \right\rangle_{\text{po}} = -P_0 \times \frac{\exp(x_0 - x_c) - 1}{\exp(x_0) - 1} \times \frac{(x_c/2)^{1/2} \exp(x_c/2) K_0(x_c/2)}{\sqrt{\pi/2}}. \quad (1)$$

Here,  $K_0(x)$  is the modified Bessel function of zeroth order,  $P_0 = 3.54 \times 10^{11} \times [\hbar\omega_{\text{LO}}(\text{meV})]^{3/2} \times (m^*/m_0)^{1/2} \times (\varepsilon_\infty^{-1} - \varepsilon_s^{-1})\text{eV/s}$ ,  $x_c = \hbar\omega_{\text{LO}}/k_B T_c$ , and  $x_0 = \hbar\omega_{\text{LO}}/k_B T_l$ .  $m^*$  is the carrier effective mass,  $\varepsilon_s$  ( $\varepsilon_\infty$ ) is the static (optical) dielectric constant, and  $\hbar\omega_{\text{LO}}$  is the longitudinal optical phonon energy. Parameters were taken from Ref. [31]. The carrier effective mass was assumed to be the electron effective mass because the energy dissipation rate for electrons is much slower

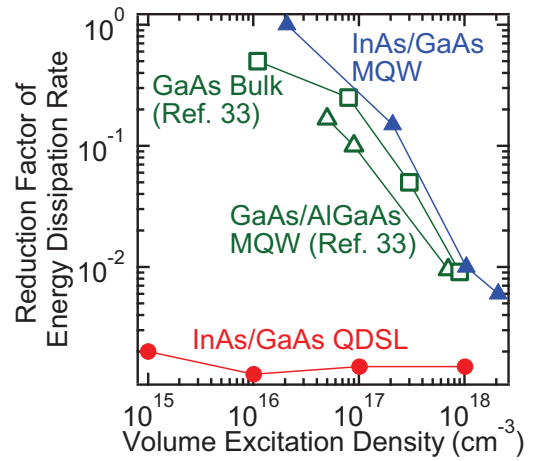


FIG. 3. Reduction factor of the HC energy dissipation rate, obtained from Fig. 2 as a function of the excitation photon density. Closed red circles and blue triangles are the results for the InAs/GaAs QDSLs and MQWs, respectively. Green symbols are the reported results for the GaAs bulk crystal and GaAs/AlGaAs MQWs, for sub-barrier excitation [33].

than that for holes [32]. The HC cooling dynamics were given by  $T_c(t) = T_0 - (C/3k_B) \int_0^t \langle dE/dt \rangle dt$  [30]. Here,  $T_0$  is the initial carrier temperature and  $C$  is the phenomenological reduction factor for the HC energy dissipation rate caused by hot phonons, carrier-carrier scattering, and carrier screening;  $C$  represents the extent of reduction in the HC energy dissipation rate compared with that owing to carrier-phonon scattering processes in the bulk crystal. On the other hand, the value of  $C$  used in this study was the reciprocal of the energy-loss rate reduction factor  $\alpha$  in Ref. [33]; therefore, the *net* HC cooling rate decreased with decreasing the  $C$ . The dashed lines in Fig. 2 represent the calculated curves with the fitting parameters of the initial carrier temperature  $T_0$  and the reduction factor  $C$ . For all excitation photon densities, the calculation correctly captured the HC cooling dynamics.

Figure 3 summarizes the reduction factor of the HC energy dissipation rate, obtained from Fig. 2 as a function of the volume excitation density. Closed red circles and blue triangles are the results for the InAs/GaAs QDSLs and MQWs, respectively. Open green symbols are the reported results for the GaAs bulk crystal (squares) and GaAs/AlGaAs MQWs (triangles), for sub-barrier excitation [33]. Our results for the InAs/GaAs MQWs for the supra-barrier excitation exhibit a trend that is similar to that for the GaAs/AlGaAs MQWs for sub-barrier excitation. This indicates that the carrier temperature has been correctly evaluated for supra-barrier excitation in this study. On the other hand, the reduction factor  $C$  monotonically decreased with increasing the excitation density, owing to the nonequilibrium hot optical phonons [32]. We assumed in Eq. (1) that the phonon occupation number is equal to that at the lattice temperature. However, the nonequilibrium optical phonon population is created with increasing the excitation photon density, leading to the reabsorption of phonons; hence, there is a reduction in the net energy-dissipation rate [34]. In contrast, the reduction factor in the InAs/GaAs QDSLs is more than one order of magnitude smaller and is almost

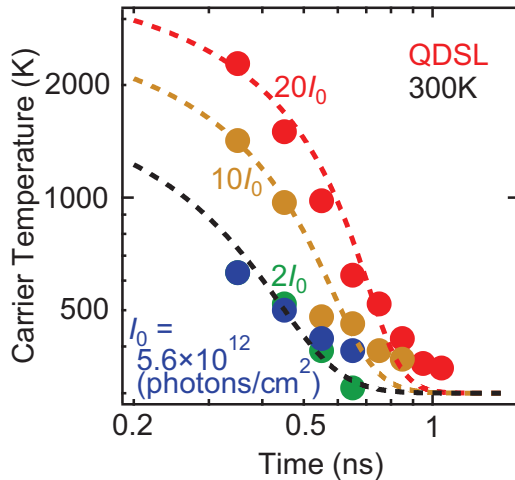


FIG. 4. HC cooling dynamics in the InAs/GaAs QDSLs for various excitation photon densities at 300 K. The dashed lines represent the calculated curves.

independent of the excitation density. Here, the reduction factor  $C$  of 0.001 resulted in the HC energy dissipation rate of  $\sim 77$  meV/ns at the carrier temperature of 1000 K. The decrease in the reduction factor results from the restrictions of phase space and energy-momentum conservation in the scattering processes in quasi-one-dimensional systems [18–21]. Furthermore, the excitation-photon-density independent reduction factor suggests the reduced efficiency of carrier-carrier scattering [19].

Finally, we performed a measurement at room temperature in the InAs/GaAs QDSLs. The PL spectrum was satisfactorily captured by the calculation accounting for the Boltzmann factor, the one-dimensional density of states, inhomogeneous broadening of the QDSLs, and homogeneous broadening at

300 K, just by changing the carrier temperature as reported in Ref. [23]. Figure 4 summarizes the HC cooling dynamics in the InAs/GaAs QDSLs for various excitation photon densities at 300 K. The calculation satisfactorily captured the HC cooling dynamics at the lattice temperature of 300 K. The reduction factor at 300 K increased by one order of magnitude relative to that at 3 K, ranging from 0.014 to 0.018. This indicates that hot nonequilibrium phonons yield slow HC cooling at 3 K in the InAs/GaAs QDSLs. Besides, the reduction factor was almost independent of the excitation photon density even at 300 K, suggesting the reduced efficiency of carrier-carrier scattering.

#### IV. SUMMARY

In conclusion, we have studied the HC cooling dynamics in the InAs/GaAs QDSLs by using time-resolved PL spectroscopy. High carrier temperature ( $>1000$  K) was demonstrated in the InAs/GaAs QDSLs owing to the one-dimensional density of states. According to the HC cooling dynamics, the HC energy dissipation rate in the InAs/GaAs MQWs decreased with increasing excitation photon density, as previously reported. Conversely, the HC energy dissipation rate in the InAs/GaAs QDSLs was more than one order of magnitude smaller than that in the MQWs, resulting from the restrictions of phase space and energy-momentum conservation in the scattering processes. Furthermore, the HC energy dissipation rate in the InAs/GaAs QDSLs was almost independent of the excitation photon density, owing to the reduced efficiency of carrier-carrier scattering.

#### ACKNOWLEDGMENTS

This work was partially supported by the Incorporated Administrative Agency New Energy and Industrial Technology Development Organization (NEDO), Japan. Y.H. was supported by the Kansai Research Foundation for Technology Promotion, Japan.

- 
- [1] R. T. Ross and A. J. Nozik, *J. Appl. Phys.* **53**, 3813 (1982).
  - [2] P. Würfel, *Sol. Energy Mater. Sol. Cells* **46**, 43 (1997).
  - [3] D. J. Farrell, Y. Takeda, K. Nishikawa, T. Nagashima, T. Motohiro, and N. J. Ekins-Daukes, *Appl. Phys. Lett.* **99**, 111102 (2011).
  - [4] S. Saeed, E. M. L. D. de Jong, K. Dohnalova, and T. Gregorkiewicz, *Nat. Commun.* **5**, 4665 (2014).
  - [5] P. Singhal and H. N. Ghosh, *Chem. Eur. J.* **21**, 4405 (2015).
  - [6] Y.-F. Lao, A. G. U. Perera, L. H. Li, S. P. Khanna, E. H. Linfield, and H. C. Liu, *Nat. Photon.* **8**, 412 (2014).
  - [7] C. V. Shank, R. L. Fork, R. F. Leheny, and J. Shah, *Phys. Rev. Lett.* **42**, 112 (1979).
  - [8] M. Bernardi, D. Vigil-Fowler, J. Lischner, J. B. Neaton, and S. G. Louie, *Phys. Rev. Lett.* **112**, 257402 (2014).
  - [9] G. Conibeer, N. Ekins-Daukes, J.-F. Guillemoles, D. König, E.-C. Cho, C.-W. Jiang, S. Shrestha, and M. Green, *Sol. Energy Mater. Sol. Cells* **93**, 713 (2009).
  - [10] M. Achermann, A. P. Bartko, J. A. Hollingsworth, and V. I. Klimov, *Nat. Phys.* **2**, 557 (2006).
  - [11] A. Pandey and P. Guyot-Sionnest, *Science* **322**, 929 (2008).
  - [12] G. J. Conibeer, D. König, M. A. Green, and J. F. Guillemoles, *Thin Solid Films* **516**, 6948 (2008).
  - [13] G. Conibeer, S. Shrestha, S. Huang, R. Patterson, H. Xia, Y. Feng, P. Zhang, N. Gupta, M. Tayebjee, S. Smyth, Y. Liao, S. Lin, P. Wang, X. Dai, and S. Chung, *Sol. Energy Mater. Sol. Cells* **135**, 124 (2015).
  - [14] P. Han and G. Bester, *Phys. Rev. B* **91**, 085305 (2015).
  - [15] A. L. Bris and J.-F. Guillemoles, *Appl. Phys. Lett.* **97**, 113506 (2010).
  - [16] L. C. Hirst, R. J. Walters, M. F. Führer, and N. J. Ekins-Daukes, *Appl. Phys. Lett.* **104**, 231115 (2014).
  - [17] J. Rodière, L. Lombez, A. L. Corre, O. Durand, and J.-F. Guillemoles, *Appl. Phys. Lett.* **106**, 183901 (2015).
  - [18] R. Cingolani, H. Lage, L. Tapfer, H. Kalt, D. Heitmann, and K. Ploog, *Phys. Rev. Lett.* **67**, 891 (1991).
  - [19] L. Rota, F. Rossi, P. Lugli, and E. Molinari, *Phys. Rev. B* **52**, 5183 (1995).

- [20] M. Oestreich, W. W. Rühle, H. Lage, D. Heitmann, and K. Ploog, *Phys. Rev. Lett.* **70**, 1682 (1993).
- [21] R. Kumar, A. S. Vengurlekar, A. Venu Gopal, T. Mélin, F. Laruelle, B. Etienne, and J. Shah, *Phys. Rev. Lett.* **81**, 2578 (1998).
- [22] C. Pryor, *Phys. Rev. B* **57**, 7190 (1998).
- [23] D. Watanabe, N. Kasamatsu, Y. Harada, and T. Kita, *Appl. Phys. Lett.* **105**, 171904 (2014).
- [24] A. Takahashi, T. Ueda, Y. Bessho, Y. Harada, T. Kita, E. Taguchi, and H. Yasuda, *Phys. Rev. B* **87**, 235323 (2013).
- [25] N. Kasamatsu, T. Kada, A. Hasegawa, Y. Harada, and T. Kita, *J. Appl. Phys.* **115**, 083510 (2014).
- [26] S. Seidl, M. Kroner, C. Lux, A. W. Holleitner, K. Karrai, R. J. Warburton, A. Badolato, and P. M. Petroff, *Appl. Phys. Lett.* **92**, 153103 (2008).
- [27] T. Kada, S. Asahi, T. Kaizu, Y. Harada, T. Kita, R. Tamaki, Y. Okada, and K. Miyano, *Phys. Rev. B* **91**, 201303(R) (2015).
- [28] R. Heitz, T. R. Ramachandran, A. Kalburge, Q. Xie, I. Mukhametzhanov, P. Chen, and A. Madhukar, *Phys. Rev. Lett.* **78**, 4071 (1997).
- [29] L. C. Hirst, H. Fujii, Y. Wang, M. Sugiyama, and N. J. Ekins-Daukes, *IEEE J. Photovolt.* **4**, 244 (2014).
- [30] J. Shah and R. F. Leheny, in *Semiconductors Probed by Ultrafast Laser Spectroscopy*, edited by R. R. Alfano (Academic, Orlando, 1984), Vol. 1, Chap. 2.
- [31] S. Adachi, *Properties of Group-IV, III-V and II-VI Semiconductors* (Wiley, Chichester, 2005).
- [32] J. Shah, A. Pinczuk, A. C. Gossard, and W. Wiegmann, *Phys. Rev. Lett.* **54**, 2045 (1985).
- [33] K. Leo, W. W. Rühle, H. J. Queisser, and K. Ploog, *Phys. Rev. B* **37**, 7121 (1988).
- [34] J. Shah, *Ultrafast Spectroscopy of Semiconductors and Semiconductor Nanostructures*, 2nd ed. (Springer-Verlag, New York, 1999), Chap. 4.